

Doubly periodic progressive permanent waves in deep water

By P. J. BRYANT

Mathematics Department, University of Canterbury, Christchurch, New Zealand

(Received 12 July 1984 and in revised form 2 May 1985)

The Stokes wave is generalized to progressive waves in deep water which are periodic in two orthogonal directions, and are steady relative to a frame of reference moving in one of these directions. These doubly periodic waves are nonlinear at their lowest approximation, and are calculated from the nonlinear equations for irrotational motion in deep water. It is shown how doubly periodic waves of small but finite wave slope may be calculated also from the nonlinear Schrödinger equation. The three-dimensional paths of particles on the free surface of a doubly periodic wave are found, and the interesting property is demonstrated that the mean particle paths differ from the direction of advance of the wave crests. The upper boundary of occurrence of doubly periodic waves at the smaller wavelength ratios is identified with the stability boundary for Stokes waves. The investigation aims to provide a closer approximation than Stokes waves to local wave structures on the ocean.

1. Introduction

The gravity-wave motion on the ocean surface consists of waves, generated at a number of sources, which interact and decay as they propagate across the surface. The local-ocean-wave spectrum has peaks, therefore, which may be identified with wavetrains propagating in different directions. The Stokes wave is a periodic wavetrain of symmetric permanent shape propagating in one direction for which the water-surface displacement is described by

$$\eta = \sum_{k=0}^{\infty} a_k \cos k(x-ct). \quad (1.1)$$

This Fourier cosine series, with constant Fourier amplitudes a_k , has permanent shape in a frame of reference moving with the wave velocity c in the x -direction. The present investigation is concerned with generalizing the Stokes wave to progressive waves of permanent shape which are periodic in two horizontal directions.

A doubly periodic progressive permanent wave is described by

$$\eta = \sum_{j=0}^{\infty} \sum_{k=-\infty}^{\infty} a_{jk} \cos \left\{ \frac{j}{r} [(x-ct) \cos \alpha + y \sin \alpha] + k[(x-ct) \cos \beta + y \sin \beta] \right\}, \quad (1.2)$$

a double Fourier cosine series with constant Fourier amplitudes a_{jk} , which has permanent shape in a frame of reference moving with velocity c in the x -direction. This wave is periodic in the two oblique directions defined by $x \cos \alpha + y \sin \alpha = \text{constant}$, and $x \cos \beta + y \sin \beta = \text{constant}$. It is composed of two wavetrains of wavelength ratio r propagating at angles α and β to the x -direction together with their nonlinear interaction. The permanent shape is equivalent to the two wavetrains being locked together in the x -direction.

The locking of the two wavetrains can occur only if the nonlinear dispersion relation for gravity waves is applicable, with dependence on wave amplitude as well as wavelength. This property implies that doubly periodic waves are nonlinear at their lowest approximation. The investigation of long-crested waves by Roberts & Peregrine (1983), using a perturbation expansion that appears to be linear at its lowest approximation, is in fact nonlinear there because it contains a wave amplitude in the linear solution that is determined by a secularity condition at the third order.

Calculations of doubly periodic permanent waves have been made by Saffman & Yuen (1980) as bifurcations of Stokes waves. They obtained two forms of wave solution, described as symmetrical and skewed. The symmetrical form is progressive in the x -direction and standing in the y -direction. The skewed form corresponds to (1.2) with $\beta = 0$, it is progressive in the x -direction, and is doubly periodic in the y -direction and in a direction $\frac{1}{2}\pi + \alpha$ with the x -axis (Saffman & Yuen 1980, §4, with r, α above related to their p, q by $(1/r) \cos \alpha = p$, $(1/r) \sin \alpha = q$). The undisturbed Stokes wave in their formulation propagates in the x -direction, when it is described by the waveband $j = 0$ in (1.2) with $\beta = 0$, and the modulation is represented by the wave components with $k = 0$, $j > 0$ in this equation. Their use of the Zakharov equation led to the neglect of interactions between higher harmonics of the undisturbed Stokes wave and the modulations, equivalent in (1.2) to $a_{jk} = 0$ for $j > 0$, $|k| > 1$. The bifurcation analysis shows that doubly periodic waves do occur in the neighbourhood of Stokes waves. The present investigation continues the analysis to fully nonlinear doubly periodic waves by avoiding the restrictions involved in calculating doubly periodic waves as weakly nonlinear perturbations to Stokes waves.

Meiron, Saffman & Yuen (1982) and Roberts & Schwartz (1983) made more accurate calculations of the symmetrical progressive-standing waves. Their method is similar to that described below (§2), except that it is based on collocation rather than on Fourier transforms. Their calculations complement the present investigation, because progressive-standing waves may occur near the shore, but on the open ocean the waves are more likely to be completely progressive. The present Fourier-transform method is preferred to collocation because it is efficient numerically and it provides immediate complete information about the spectral composition of the wave solutions. Ma (1982) used a more general form of the Zakharov equation to calculate bifurcations to Stokes waves. His representation is the particular case of (1.2) with $\beta = 0$ for which $a_{jk} = 0$, $j > 1$, equivalent to linearization in the modulation. Martin (1982) found symmetrical and skewed wave solutions of the nonlinear Schrödinger equation having the same form as those of Saffman & Yuen (1980).

Roberts (1983) used a perturbation expansion in the wave slope to calculate short-crested symmetrical progressive-standing wave solutions of Laplace's equation with the nonlinear free-surface boundary conditions ((2.1) below). This approach complements the solutions by collocation referred to above, and was used also by Roberts & Peregrine (1983) to calculate long-crested progressive-standing wave solutions. The latter investigation is discussed in §§4, 5 below.

The doubly periodic waves calculated here are the simple case given by $\alpha = \frac{1}{2}\pi$, $\beta = 0$ in (1.2), namely

$$\eta = \sum_{j=0}^{\infty} \sum_{k=-\infty}^{\infty} a_{jk} \cos \left\{ \frac{j}{r} y + k(x-ct) \right\}, \quad (1.3)$$

which are periodic in the x - and y -directions. An example of such a wave is sketched in perspective in figure 1, showing 4 wavelengths in the x -direction and 2 wavelengths in the y -direction, with $r = 4$. The wave has permanent shape relative to a frame of

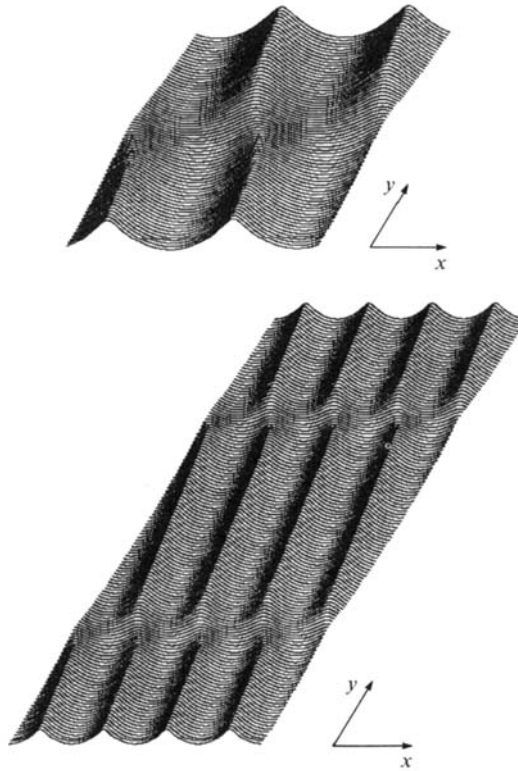


FIGURE 1. Perspective view of doubly periodic waves with $\epsilon = 0.5$, $r = 4$, showing 4 wavelengths in the x -direction and 2 wavelengths in the y -direction, and a detailed view of the ends of the crests. Vertical magnification 2.

reference moving in the x -direction, and the straight-crested part of the wave progresses at 10.5° to the x -direction. It is demonstrated in §6 how the particle paths are three-dimensional with a mean direction for the straight-crested parts which is inclined at only 0.8° to the x -direction. The structure at the ends of the crests is shown in greater detail in the upper part of the figure. The minimum wave height (trough to crest) at the ends of the crests is 0.53 of the maximum wave height of the straight-crested part.

Attention is drawn to the similarity in appearance between figure 1 and the wave patterns generated experimentally by Su (1982, figure 4). His wave patterns are part of an evolving wavefield, rather than the steady wave patterns calculated here. Nevertheless, the qualitative similarity gives confidence in the physical relevance of doubly periodic waves.

The motivation for the present investigation is that of setting up a particular more-realistic local nonlinear model of the open ocean surface than is given by the Stokes wave. The model is used to calculate relevant properties, such as the form of the Stokes drift on a doubly periodic ocean surface. The method used here may be generalized to the calculation of further specific nonlinear ocean wave structures (Bryant 1984), because it makes no explicit approximations for the nonlinear properties of the ocean surface.

2. Calculation of doubly periodic waves

The set of equations describing gravity waves in inviscid irrotational motion in deep water is

$$\phi_{xx} + \phi_{yy} + \phi_{zz} = 0, \quad z < \epsilon\eta(x, y, t), \quad (2.1a)$$

$$\phi_x, \phi_y, \phi_z \rightarrow 0, \quad z \rightarrow -\infty, \quad (2.1b)$$

$$\eta_t - \phi_z + \epsilon\eta_x \phi_x + \epsilon\eta_y \phi_y = 0, \quad z = \epsilon\eta(x, y, t), \quad (2.1c)$$

$$\eta + \phi_t + \frac{1}{2}\epsilon(\phi_x^2 + \phi_y^2 + \phi_z^2) = 0, \quad z = \epsilon\eta(x, y, t). \quad (2.1d)$$

The dimensional variables are the water-surface displacement $a\eta$, the velocity potential $(gl)^{\frac{1}{2}}a\phi$, and $lx, ly, lz, (l/g)^{\frac{1}{2}}t$, where a is the maximum wave height $\eta(0, 0, 0)$, $2\pi l$ is the wavelength in the x -direction, and $\epsilon = a/l$ is a measure of wave slope. The origin of the coordinates lies in the mean free surface with the z -axis vertically upwards.

The non-dimensional description of the simple doubly periodic permanent wave (1.3) is

$$\eta = \sum_{j=0}^J \sum_{k=k_1(j)}^{k_2(j)} a_{jk} \cos \left\{ \frac{j}{r} y + k(x-ct) \right\}, \quad (2.2a)$$

which is a wavetrain with wavelengths $2\pi l$ in the x -direction, $2\pi r l$ in the y -direction, whose shape is steady relative to a frame of reference moving with velocity $c(gl)^{\frac{1}{2}}$ in the x -direction. The bounds of summation are determined numerically by trial and error so that the set of amplitudes a_{jk} includes all those amplitudes greater in magnitude than some small prescribed value (usually 10^{-4}). Since η is chosen to have a zero mean, the lower bound $k_1(0)$ may be set equal to 1. Other lower bounds $k_1(j)$, $j > 0$ may be negative. The associated solution of Laplace's equation (2.1a) is

$$\phi = \sum_{j=0}^J \sum_{k=k_1(j)}^{k_2(j)} b_{jk} \exp \left\{ \left(\left(\frac{j}{r} \right)^2 + k^2 \right)^{\frac{1}{2}} z \right\} \sin \left\{ \frac{j}{r} y + k(x-ct) \right\}. \quad (2.2b)$$

The set of amplitudes a_{jk} , b_{jk} (all j, k) and the non-dimensional wave velocity c are unknown functions of the wave slope parameter ϵ and the wavelength ratio r .

Equations (2.2) describe one particular family of doubly periodic waves, probably the simplest family. These equations are numerically complete in the sense that they include a complete set of wave components, greater in magnitude than some small prescribed value, which are generated by the nonlinear interactions contained in (2.1c, d).

The solution method is the same as that applied to oblique wave groups in deep water (Bryant 1984), where more details about the method may be found. Equations (2.2a, b) are substituted into (2.1c, d), with c_{jk} denoting the cosine in (2.2a) and s_{jk} the sine in (2.2b), giving

$$\begin{aligned} F = & \sum_j \sum_k \left\{ kca_{jk} s_{jk} - \left(\left(\frac{j}{r} \right)^2 + k^2 \right)^{\frac{1}{2}} b_{jk} \exp \left\{ \epsilon \left(\left(\frac{j}{r} \right)^2 + k^2 \right)^{\frac{1}{2}} \eta \right\} s_{jk} \right\} \\ & - \epsilon \left[\sum_j \sum_k ka_{jk} s_{jk} \right] \left[\sum_j \sum_k kb_{jk} \exp \left\{ \epsilon \left(\left(\frac{j}{r} \right)^2 + k^2 \right)^{\frac{1}{2}} \eta \right\} c_{jk} \right] \\ & - \epsilon \left[\sum_j \sum_k \frac{j}{r} a_{jk} s_{jk} \right] \left[\sum_j \sum_k \frac{j}{r} b_{jk} \exp \left\{ \epsilon \left(\left(\frac{j}{r} \right)^2 + k^2 \right)^{\frac{1}{2}} \eta \right\} c_{jk} \right] = 0, \quad (2.3a) \end{aligned}$$

$$\begin{aligned}
G = & \sum_j \sum_k \left\{ a_{jk} c_{jk} - k c b_{jk} \exp \left\{ \epsilon \left(\left(\frac{j}{r} \right)^2 + k^2 \right)^{\frac{1}{2}} \eta \right\} c_{jk} \right\} \\
& + \frac{1}{2} \epsilon \left(\sum_j \sum_k k b_{jk} \exp \left\{ \epsilon \left(\left(\frac{j}{r} \right)^2 + k^2 \right)^{\frac{1}{2}} \eta \right\} c_{jk} \right)^2 \\
& + \frac{1}{2} \epsilon \left(\sum_j \sum_k \frac{j}{r} b_{jk} \exp \left\{ \epsilon \left(\left(\frac{j}{r} \right)^2 + k^2 \right)^{\frac{1}{2}} \eta \right\} c_{jk} \right)^2 \\
& + \frac{1}{2} \epsilon \left(\sum_j \sum_k \left(\left(\frac{j}{r} \right)^2 + k^2 \right)^{\frac{1}{2}} b_{jk} \exp \left\{ \epsilon \left(\left(\frac{j}{r} \right)^2 + k^2 \right)^{\frac{1}{2}} \eta \right\} s_{jk} \right)^2 = 0, \quad (2.3b)
\end{aligned}$$

where

$$\exp \left\{ \epsilon \left(\left(\frac{j}{r} \right)^2 + k^2 \right)^{\frac{1}{2}} \eta \right\} = \exp \left\{ \epsilon \left(\left(\frac{j}{r} \right)^2 + k^2 \right)^{\frac{1}{2}} \sum_p \sum_q a_{pq} c_{pq} \right\}.$$

Also

$$H = \sum_j \sum_k a_{jk} - 1 = 0 \quad (2.3c)$$

because the maximum non-dimensional surface displacement $\eta(0, 0, 0)$ is taken to be 1. Equations (2.3a, b) are calculated at a grid of points in $x-ct, y/r$ space, and with fast Fourier transforms are reduced numerically to

$$F = \sum_m \sum_n F_{mn} s_{mn} = 0, \quad G = \sum_m \sum_n G_{mn} c_{mn} = 0, \quad (2.4a, b)$$

from which

$$F_{mn} = G_{mn} = 0, \quad \text{all } m, n. \quad (2.5)$$

The Fourier coefficients F_{mn}, G_{mn} are nonlinear functions of a_{jk}, b_{jk} (all j and k) and c for given ϵ and r . Fourier transforms are calculated for the derivatives of F, G and H with respect to a_{jk}, b_{jk} (all j and k) and c . Newton's method is then used in the Fourier transform space to calculate a_{jk}, b_{jk} (all j and k) and c as solutions of (2.3a, b, c) on the grid of points used for the Fourier transforms. All calculations were performed in double precision on a Prime 750 computer, with subroutines adapted from the Harwell Subroutine Library.

3. Occurrence of doubly periodic waves

Doubly periodic waves are calculated as functions of ϵ and r by making step-by-step changes in either ϵ or r to find new solutions from old solutions. For any given value of the wavelength ratio r , doubly periodic waves of the form described by (2.2) exist for values of the wave-slope parameter ϵ greater than some positive minimum. As ϵ approaches the minimum value from above, the doubly periodic waves tend towards a Stokes wave propagating in a direction $\theta_0 = \tan^{-1}(1/r)$ with the x -direction. The wavelength $2\pi l_0$ of the Stokes waves is given by

$$l_0 = l \cos \theta_0 = \frac{lr}{(r^2 + 1)^{\frac{1}{2}}}, \quad (3.1)$$

and if the trough-to-crest height of the Stokes wave is denoted by $2a_0$, a more appropriate wave-slope parameter for the Stokes wave is

$$\epsilon_0 = a_0/l_0. \quad (3.2)$$

As ϵ tends to the minimum value from above, the Jacobian in Newton's method increases in magnitude, making it possible to calculate the minimum value of ϵ and

the Stokes wave solution there with accuracy. In contrast, calculation of the maximum value of ϵ for any given r is approximate because the Jacobian in Newton's method decreases in magnitude as this limit is approached, and because the series representation for the velocity potential may fail to converge.

Although the minimum value of ϵ is a point of bifurcation between doubly periodic waves and Stokes waves, the solution branch with r kept constant may be followed through the bifurcation point to the Stokes wave solutions at values of ϵ below the minimum for doubly periodic waves. The Jacobian on this solution branch increases in magnitude as ϵ decreases, except for a local decrease in magnitude near the point of bifurcation itself. This local decrease may be missed unless the stepsize in ϵ between consecutive calculations is sufficiently small. If this solution branch is followed upwards, beginning with the Stokes wave solutions below the minimum value for doubly periodic waves, the Jacobian changes sign at the bifurcation point, and the solutions continue on a Stokes-wave-solution branch above the bifurcation point.

For values of ϵ greater than the minimum, a more appropriate waveslope parameter may be defined from the wave height and wavelength of the straight-crested parts of the doubly periodic wave. The wave height $2a_0$ and wavelength $2\pi l_0$ are both determined from the wave solution once it has been calculated for the given values of ϵ and r . In the example in figure 1, for which $\epsilon = 0.5$, $r = 4$, these parameters are $a_0 = 0.394l$, $l_0 = 0.983l$, making $\epsilon_0 = 0.40$. The minimum value of ϵ for $r = 4$ is 0.276, when the Stokes wave there has a wave-slope parameter $\epsilon_0 = 0.250$. The maximum value of ϵ when $r = 4$ is 0.584 approximately, for which the straight-crested parts of the wave have a wave-slope parameter $\epsilon_0 = 0.437$.

The basic geometric unit of the doubly periodic wave structure described by (2.2) is a rectangle of sides $2\pi l$ in the x -direction and $2\pi r l$ in the y -direction. The angle $\tan^{-1}(1/r)$ in this rectangle equals the direction of propagation θ_0 of the Stokes wave at the minimum value of ϵ for the given value of r . The wave-slope parameter ϵ_0 normal to the straight-crested parts of the wave is a more descriptive amplitude parameter than the wave-slope parameter ϵ in the x -direction. For these reasons, the region of occurrence of the doubly periodic waves is sketched in figure 2 in terms of θ_0 and ϵ_0 .

The lower curve in figure 2 has been calculated to within the accuracy of the figure for values of θ_0 up to about 60° . Wave resonances become significant at greater angles (§7), where the doubly periodic wave solutions do not appear to be physically relevant. The upper curve in figure 2 is everywhere approximate for the reasons stated above. It could not be extended to values of θ_0 below about 5° because the number of wave components required to find solutions there exceeded the computing capacity available. The region of occurrence is discussed in three parts, small wave slopes (§5), large wave slopes with θ_0 small (§6), and large wave slopes with θ_0 large (§7).

4. Nonlinear Schrödinger equation

The nonlinear Schrödinger equation for wave motion on the surface of deep water, using the non-dimensional notation defined in §2, is

$$i(A_t + \frac{1}{2}A_x) - \frac{1}{8}A_{xx} + \frac{1}{4}A_{yy} - \frac{1}{2}\epsilon^2 |A|^2 A = 0, \quad (4.1a)$$

where

$$\eta = \text{Re} \{A(x, y, t) \exp i(x-t)\}. \quad (4.1b)$$

The equation is valid for waves of small but finite wave slope ϵ , for which the amplitude function $A(x, y, t)$ is a slowly varying function of x , y and t . The latter

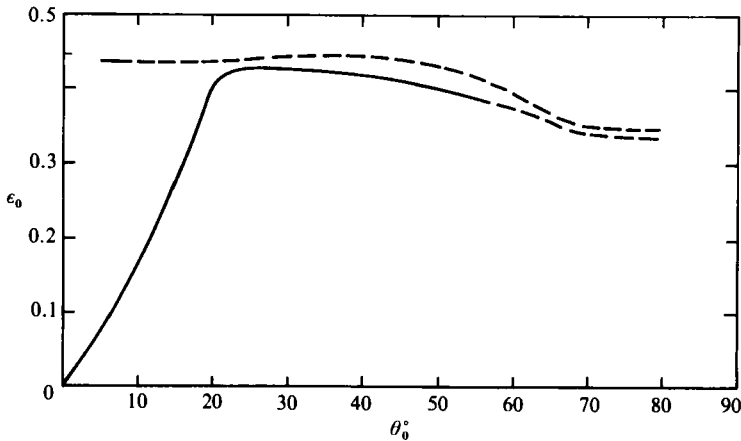


FIGURE 2. The region of occurrence of doubly periodic waves in terms of the angle θ_0 of the basic rectangle and the wave slope parameter ϵ_0 . The lower boundary is shown as a solid curve where it has been calculated within the precision of the figure. The maximum value of ϵ_0 for Stokes waves is marked on the axis.

condition is equivalent to the Fourier decomposition of η having a single narrow peak in two-dimensional wavenumber space near the wave component of wavenumber 1 in the x -direction. These conditions are satisfied for doubly periodic waves near the origin in figure 2, implying that these waves should be modelled by (4.1). The analysis below is similar to that derived by Roberts & Peregrine (1983, appendix), but is repeated here to demonstrate that the numerical solutions by the method of §2 are consistent with the corresponding solutions of the nonlinear Schrödinger equation.

The amplitude function for the simple doubly periodic waves described by (2.2) is a non-zero function dependent on y and t alone, $A(y, t)$. Equation (4.1a), with the substitution

$$A(y, t) = F(y) \exp \{i\Phi(y) - i\alpha t\} \quad (4.2)$$

(F, Φ, α real), followed by cancellation of the exponential functions, has real and imaginary parts

$$F_{yy} - F\Phi_y^2 + 4\alpha F - 2F^3 = 0, \quad F\Phi_{yy} + 2F_y\Phi_y = 0. \quad (4.3a, b)$$

Equation (4.3b) integrates to

$$F^2\Phi_y = B, \quad (4.4)$$

where B is an arbitrary constant. After substitution for Φ_y , (4.3a) becomes

$$F_{yy} - \frac{B^2}{F^3} + 4\alpha F - 2F^3 = 0 \quad (4.5a)$$

which integrates to

$$F_y^2 = F^4 - 4\alpha F^2 - \frac{B^2}{F^2} + C, \quad (4.5b)$$

where C is an arbitrary constant.

Equation (4.5b) with $B = 0$ has no solutions describing a periodic oscillation of $F(y)$ between positive extrema F_1, F_2 . If F_y has zeroes at $F = F_1, F_2$, (4.5b) with $B = 0$ has the form

$$F_y^2 = (F_1^2 - F^2)(F_2^2 - F^2), \quad (4.6)$$

which has no real solutions with $F_1 < F < F_2$. If B is non-zero, (4.5b) with a suitable choice of α , B , and C can have the form

$$F_y^2 = \frac{(F^2 - F_0^2)(F_1^2 - F^2)(F_2^2 - F^2)}{F^2}, \quad (4.7)$$

where $0 < F_0 < F_1 < F_2$. Equation (4.7) does have periodic solutions for which $F_0 \leq F \leq F_1$. Hence the nonlinear Schrödinger equation (4.1a) can have solutions of the form of (4.2) with a positive periodic amplitude $F(y)$ provided that the phase $\Phi(y)$ is a monotonically increasing or monotonically decreasing function of y . The water surface displacement, (4.1b), is then

$$\eta = F(y) \cos \{x + \Phi(y) - (1 + \alpha)t\}, \quad (4.8)$$

which is a wavetrain periodic in the x -direction, slowly varying in the y -direction, that is steady relative to the frame of reference moving with a non-dimensional velocity $c = 1 + \alpha$ in the x -direction. If the wavetrain is periodic in the y -direction also, with a non-dimensional wavelength $2\pi r$, then the solution $F(y)$ of (4.5) has wavelength $2\pi r$, and from equation (4.4)

$$B \int_0^{2\pi r} F^{-2} dy = 2\pi \quad (4.9)$$

for the simplest doubly periodic wave.

Equation (4.5a) may be solved, subject to the constraint (4.9), by a numerical method which is a simplified version of that described in §2 (see also Bryant 1984, §3). Since $F(y)$ is symmetric in y with a wavelength $2\pi r$, it may be written as the Fourier cosine series

$$F(y) = \frac{1}{2}a_0 + \sum_{k=1}^N a_k \cos \frac{ky}{r}, \quad (4.10)$$

where N is determined by trial and error so that the set of amplitudes a_k includes all those greater in magnitude than some small prescribed value (10^{-5} here). The Fourier series is substituted into (4.5a), which is expanded numerically into a Fourier cosine series at given values of ϵ , r , and B , and is solved by Newton's method for the $N+1$ Fourier amplitudes a_0, a_1, \dots, a_N and the parameter α . The constant B is then changed step by step until the constraint (4.9) is satisfied.

The doubly periodic wave solutions of the nonlinear Schrödinger equation (4.1) were found to be in good agreement with the corresponding doubly periodic waves calculated from (2.1) at values of ϵ near the origin in figure 2. Some properties of the doubly periodic wave for which $\epsilon = 0.12$, $r = 10$ ($c = 1.008$, $\epsilon_0 = 0.096$, $\theta_0 = 5.71^\circ$) are sketched in figure 3. The solid curves are derived from (2.1) and the dashed curves from the nonlinear Schrödinger equation (4.1). The left-hand section shows two transverse wavelengths of the upper and lower wave envelopes, which for the nonlinear Schrödinger equation are $\pm F(y)$. The right-hand curve is two transverse wavelengths of the wave crest, given for the nonlinear Schrödinger equation by

$$x + \Phi(y) - (1 + \alpha)t = 0, \quad 1 + \alpha = c \quad (4.11)$$

in (4.8). The two solutions coincide within the precision of the figure except for the slight separation of the lower envelopes, which gives confidence in the validity of both solutions.

Roberts & Peregrine (1983) calculated long-crested water waves which progress in the x -direction, are standing waves in the transverse direction, and are doubly periodic in these two directions. They used a perturbation expansion in wave slope valid for the parameter range $\epsilon \sim \theta_0 \ll 1$ (in the present notation). Since their



FIGURE 3. Comparison of properties of the doubly periodic wave with $\epsilon = 0.12$, $r = 10$ and those of the corresponding solution of the NLS equation. On the left are two transverse wavelengths of the upper and lower envelopes (vertical magnification 20), and on the right are two transverse wavelengths of the wave crest. The dashed curve, distinguishable only on the lower envelope, is the NLS solution.

leading-order solution has no phase change with respect to the transverse variable, their equations (2.10), (2.11) for the wave amplitude are the same (apart from a scaling factor) as equations (4.5*a*, *b*) above with $B = 0$. These equations were shown to have sn solutions with envelope zeroes. Their fourth-order solutions for doubly periodic long-crested waves have envelope zeroes also. However, their analysis of the nonlinear Schrödinger equation does admit doubly periodic progressive wave solutions without envelope zeroes, suggesting that the perturbation-expansion method could be used to calculate doubly periodic progressive wave solutions without envelope zeroes, for which the leading-order solution does have a phase change with respect to the transverse variable.

5. Doubly periodic waves of small wave slope

Two properties of doubly periodic waves of small wave slope are investigated here. Reasons are sought for the right boundary of the region of occurrence of these waves in figure 2 being asymptotic to a straight line through the origin as ϵ_0 tends to zero. The form of the doubly periodic waves as the left boundary is approached, when the wavelength ratio r becomes large, is also examined.

The right boundary of the region of occurrence is asymptotic to a straight line through the origin of slope 0.877 when θ_0 is expressed in radians. This boundary is the minimum value of the wave-slope parameter ϵ_0 , for any given wavelength ratio r ($= \cot \theta_0$), at which two waves at angle θ_0 may be locked together to form a doubly periodic wave of permanent shape. The doubly periodic wave is a Stokes wave at this minimum value, whose dimensional wave velocity, as calculated by Stokes, is

$$c_0 = (gl_0)^{\frac{1}{2}} \left(1 + \frac{1}{2}\epsilon_0^2 + O(\epsilon_0^4)\right), \quad (5.1)$$

in the present notation. The non-dimensional velocity in the x -direction of a Stokes wave propagating at angle θ_0 to the x -direction, using (3.1), is therefore

$$\begin{aligned} c &= c_0 (gl)^{-\frac{1}{2}} (\cos \theta_0)^{-1} \\ &= (\cos \theta_0)^{-\frac{1}{2}} \left(1 + \frac{1}{2}\epsilon_0^2 + O(\epsilon_0^4)\right). \end{aligned} \quad (5.2)$$

This relation is fitted accurately on the whole lower boundary in figure 2.

For values of ϵ_0 slightly greater than the minimum value, the doubly periodic wave in the region of small wave slope consists of the Stokes wave at angle θ_0 locked together with a wave component of much smaller magnitude in the x -direction. For dimensional reasons, the drift velocity associated with this Stokes wave, expressed in dimensional form, may be written

$$v = \kappa c_0 \epsilon_0^2 \quad (5.3)$$

in the direction of propagation of the Stokes wave, where κ is a dimensionless constant. The non-dimensional velocity in the x -direction of the wave component propagating in this direction on top of the Stokes wave at angle θ_0 is therefore

$$\begin{aligned} c &= (v \cos \theta_0 + (gl)^{\frac{1}{2}}) (gl)^{-\frac{1}{2}} \\ &= 1 + \kappa (\cos \theta_0)^{\frac{3}{2}} \epsilon_0^2 + O(\epsilon_0^3). \end{aligned} \quad (5.4)$$

Equations (5.2) and (5.4) are the same for $\theta_0 \sim \epsilon_0 \ll 1$, expressing the locking together of the two waves into the doubly periodic wave near the right boundary, provided that

$$\epsilon_0 = (4\kappa - 2)^{-\frac{1}{2}} \theta_0 + O(\theta_0^2). \quad (5.5)$$

This equation shows that the right boundary is asymptotic to a straight line through the origin as ϵ_0 tends to zero for doubly periodic waves. The dimensionless constant κ has the value 0.825 for the straight line to take the measured slope 0.877.

Analytical reasons have been sought unsuccessfully for the dimensionless constant κ in (5.3) being 0.825. The Stokes drift velocity for fluid particles at mean level lz_0 is (Lighthill 1978, p. 280)

$$v = c_0 \epsilon_0^2 \exp(2z_0). \quad (5.6)$$

The wave component propagating in the x -direction experiences a weighted average of the particle velocities associated with the Stokes wave at levels near $z_0 = 0$, whose net effect is to cause the dimensionless constant κ to have the value found.

An example is presented of a doubly periodic wave near the left boundary of the region of small wave slope in figure 2. It tests the accuracy there of doubly periodic wave solutions of the nonlinear Schrödinger equation, and may be compared with the long-crested wave of infinite transverse wavelength calculated by Roberts & Peregrine (1983). The parameters for the example are $\epsilon = 0.1$, $r = 100$ ($c = 1.0046$, $\epsilon_0 = 0.095$, $\theta_0 = 0.57^\circ$). The solid curves on the left of figure 4 are the central one eighth of a transverse wavelength of the upper and lower envelopes (contracted 32 times). The remaining seven eighths of the transverse wavelength is a wavetrain of constant height. The minimum separation of the envelopes at the centre is 0.056 of the maximum separation. The solid curve on the right of figure 4 is the central one eighth of a transverse wavelength of a wave crest (contracted 32 times). The remaining seven eighths of the crest is a straight line inclined at 0.30° to the y -direction. The fit between the exact doubly periodic wave properties and the corresponding properties of solutions of the nonlinear Schrödinger equation is seen in figure 4 to be very good, probably because this example fits well the assumptions made in deriving the nonlinear Schrödinger equation.

The water-surface displacement of the central one eighth of a transverse wavelength is sketched in perspective in figure 5. The figure shows good qualitative agreement with the perspective drawing of the long-crested wave of infinite transverse wavelength calculated by Roberts & Peregrine (1983, figure 4). Both examples are steady relative to a frame of reference moving in the x -direction. However, their example is standing in the transverse direction, while the present example, as can be seen in figure 4, has

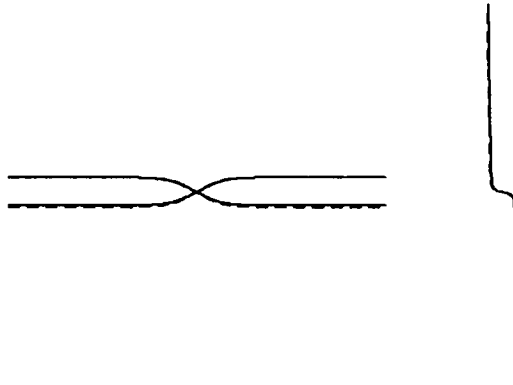


FIGURE 4. Comparison of properties of the doubly periodic wave with $\epsilon = 0.1$, $r = 100$ and those of the corresponding solution of the NLS equation. On the left is one eighth of a transverse wavelength of the upper and lower envelopes (minimum separation 0.056 of maximum separation), and on the right is one eighth of a transverse wavelength of the wave crest, all contracted 32 times in the transverse direction. The dashed curve, distinguishable only on the lower envelope, is the NLS solution.

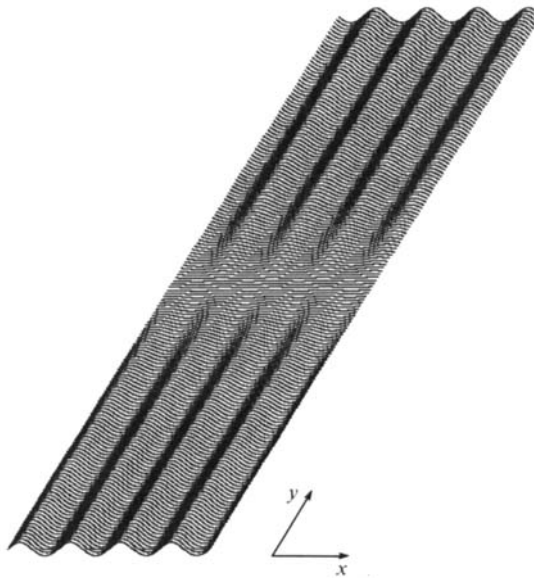


FIGURE 5. Perspective view of doubly periodic waves with $\epsilon = 0.1$, $r = 100$, showing 4 wavelengths in the x -direction and one eighth of a wavelength in the y -direction. Vertical magnification 10.

a small progressive component of velocity in the transverse direction. For this reason, a quantitative comparison is not meaningful.

The water-surface displacement and velocity potential for the present example (2.2) each contain 263 wave components in 46 wavebands ($0 \leq j \leq 45$), the wavenumber range being $-5 \leq k \leq 5$. The maximum Fourier coefficients F_{mn} , G_{mn} not included in the calculation have magnitude 2×10^{-4} . The maximum magnitude of F and G over the 128×16 points used in the final calculation is 6.8×10^{-3} , with a root-mean-square deviation of F and G from zero of 8×10^{-4} . (A computer listing of the wave components for all examples may be obtained from the author.)

6. Large wave slope with large wavelength ratio

Doubly periodic waves in the upper-left part of the region of occurrence (figure 2) are discussed here. The structure of these waves is the same as that of doubly periodic waves of small slope, namely two wavetrains locked together. However, because the wave slopes are larger, more wave components are generated by the nonlinear interactions between the two basic wave components. Attention is restricted here to the family of doubly periodic waves for which the two basic wave components are ($j = 0, k = 1$) and ($j = 1, k = 1$) in (2.2a). Two examples are presented, the first with $\epsilon = 0.05, r = 4$, and the second with $\epsilon = 0.5, r = 10$.

The doubly periodic wave with parameters $\epsilon = 0.5, r = 4$ ($\epsilon_0 = 0.400, \theta_0 = 14.04^\circ, c = 1.0903$) is sketched in perspective in figure 1. The structure at the ends of the crests is shown in more detail at the top of the figure, where the minimum wave height (trough to crest) is 0.53 of the maximum wave height of the straight-crested part. The doubly periodic wave solution of the nonlinear Schrödinger equation with the same parameters as this example was compared with the example, and found to be unsatisfactory, as is expected for this large value of ϵ . The upper envelope $F(y)$ and the phase $\Phi(y)$ were both in error at the ends of wave crests, and the lower envelope $-F(y)$ was well in error throughout the transverse wavelength. The water-surface displacement and velocity potential (2.2a, b) each contain 182 wave components in 14 wavebands ($0 \leq j \leq 13$), the wavenumber range being $-6 \leq k \leq 18$. The maximum Fourier components F_{mn}, G_{mn} not included in the calculation have magnitudes 3×10^{-4} . The maximum magnitude of F and G over the 64×32 points used in the final calculation is 6.3×10^{-3} , with a root-mean-square deviation of F and G from zero of 1.0×10^{-3} .

The projections on the (x, z) -plane of the free-surface particle paths at points initially equally spaced across one transverse wavelength are shown on the left of figure 6, and the mean-drift velocity in this direction, calculated from particle paths, is drawn on the right of the figure. Each of the fluid particles in the figure lies initially at the free surface on a transverse cross-section extending from the centre of a straight-crested part to the centre of the next straight-crested part of the wave. The mean-drift velocity in the transverse direction is uniform in y . The interesting property is that the angle of mean drift for the straight-crested part of the wave is inclined at only 0.8° to the x -direction, while the crest itself advances in a direction at 10.5° to the x -direction. The particle paths are of a spiral shape with a mean direction of advance which is oblique to the direction of advance of the wave crests containing the particles. Particle paths in two-dimensional Stokes waves are orthogonal to wave crests, but this property is not true for the three-dimensional situation in which the waves have a doubly periodic structure.

The second example is of a doubly periodic wave with parameters $\epsilon = 0.5, r = 10$ ($\epsilon_0 = 0.396, \theta_0 = 5.71, c = 1.0816$) and is sketched in perspective in figure 7. The straight-crested part of the wave progresses at 3.2° to the x -direction, and the minimum wave height (trough to crest) at the ends of the crests is 0.18 of the maximum wave height of the straight-crested part. The free-surface particle paths were found to have properties similar to those in the first example. The mean drift at the free surface in the straight-crested part of the wave is inclined at only 0.1° to the x -direction.

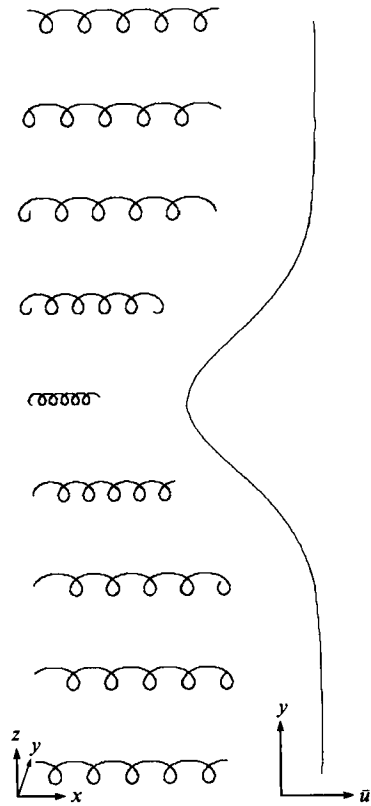


FIGURE 6. Projections on the vertical (x, z) -plane of free-surface particle paths across one transverse (y) wavelength for the doubly periodic wave with $\epsilon = 0.5$, $r = 4$, drawn to scale. On the right is the drift-velocity profile as a function of the transverse coordinate y calculated from the free-surface particle paths.

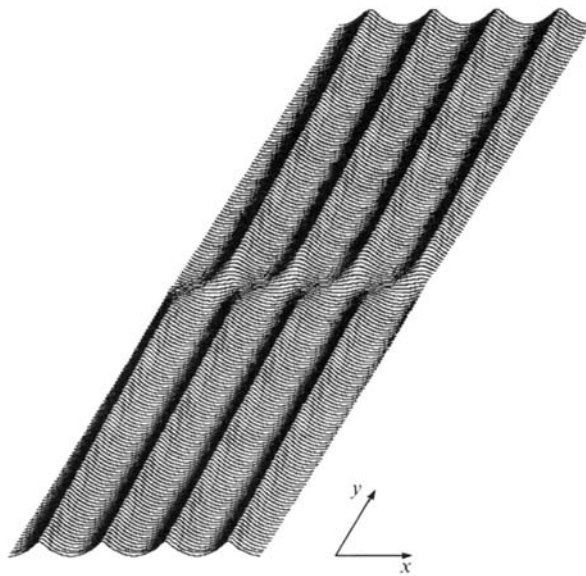


FIGURE 7. Perspective view of doubly periodic waves with $\epsilon = 0.5$, $r = 10$, showing 4 wavelengths in the x -direction and 1 wavelength in the y -direction. Vertical magnification 2.

7. Large wave slope with small wavelength ratio

There is a narrow region in figure 2 for values of θ_0 greater than about 20° , and for large wave slopes, in which doubly periodic waves were found to occur. The doubly periodic waves tend towards Stokes waves as the lower boundary of the region is approached, indicating that within the narrow region the doubly periodic waves are close approximations to Stokes waves, differing only in that other wave components of much smaller amplitude are locked together with the Stokes wave components. McLean *et al.* (1981) and McLean (1982) have calculated the regions of instability of Stokes waves to oblique perturbations, with linearization in the perturbations. The instability is associated with resonance in the sense that certain wave components lie near the linear dispersion relation. The upper boundary of the narrow region calculated here is interpreted as the nonlinear generalization of the stability boundary found by the linear stability analysis.

The Stokes wave components here are those for which $j = k$ in (2.2a). A non-dimensional rectangular coordinate system relative to the Stokes wave is defined by

$$X = x + \frac{1}{r} y, \quad Y = -\frac{1}{r} x + y, \quad (7.1)$$

for which (2.2a) becomes

$$\eta = \sum_j \sum_k a_{jk} \cos \left\{ k(X - ct) + \frac{j-k}{1+r^2} (X + rY) \right\}. \quad (7.2)$$

Linearization (McLean (1982), equation 5) restricts the Stokes wave perturbations to wave components for which

$$j - k = \pm 1 \quad (7.3)$$

in (7.2), when the perturbation wavenumbers are

$$p = \frac{1}{1+r^2}, \quad q = \frac{r}{1+r^2} \quad (7.4)$$

(p, q in McLean's notation). An example is presented in which a doubly periodic wave on the upper boundary of the narrow region is interpreted in terms of the linear stability analysis.

The doubly periodic wave of maximum wave height when $r = 0.6$ is found to have parameters $\epsilon_0 = 0.40$, $\theta_0 = 59.0^\circ$, $h/\lambda = 0.126$ (in McLean's notation), and $p = 0.74$, $q = 0.44$ from (7.4). The instability diagram for a Stokes wave with this value of the wave-slope parameter h/λ is sketched by McLean (1982, p. 322, figure 2e). The instability diagrams for smaller values of h/λ show that Stokes waves are stable to a perturbation with these values of p and q . However, at this value of h/λ , the perturbation wavenumbers p and q lie just inside the region of class II instability. Although the dominant off-diagonal wave components of this doubly periodic wave are those for which $j - k = +1$, the components for which $j - k = +2$ are of greater magnitude than those for which $j - k = -1$. The restriction (7.3) is not fully applicable therefore, suggesting that this approximate agreement with McLean's calculations is as much as can be expected.

As the wavelength ratio r is decreased further, equivalent to θ_0 increasing, certain off-diagonal wave components increase relative to other wave components because of their nearness to linear resonance. Examination of McLean's instability diagrams shows that class I instabilities contribute at the lower values of the wave-slope parameter applicable here. These doubly periodic waves have not been investigated

in detail because of the doubtful physical relevance when their wave crests are inclined at large angles to the direction in which the waves have constant shape. It is difficult to visualize a natural generating mechanism whose coherence extends over such large angles.

8. Generalizations

The doubly periodic progressive waves studied here are probably the simplest of their kind. They are periodic in two orthogonal directions, and are steady relative to a frame of reference moving in one of these directions. In the course of calculating the waves, other solution branches were also found. One branch consists of waves dominated by the wave components for which $(j = 0, k = 1)$ and $(j = 2, k = 1)$, with a much smaller $(j = 1, k = 1)$ component. These doubly periodic waves have a similar appearance to those described in §§5 and 6 except that a modulation of twice the transverse wavelength is locked in with them. Another branch consists of waves dominated by wave components of unequal amplitude for which $(j = 1, k = 1)$ and $(j = 1, k = -1)$. These doubly periodic waves are more symmetric in appearance than those described here.

Some calculations have been made on doubly periodic waves which are periodic in two non-orthogonal directions. The skewed doubly periodic waves of Saffman & Yuen (1980), for which

$$\eta = \sum_j \sum_k a_{jk} \cos \left\{ \frac{j}{r} [(x-ct) \cos \alpha + y \sin \alpha] + k(x-ct) \right\}, \quad (8.1)$$

were calculated and extended to larger wave slopes than the Zakharov equation permits. The method of calculation was a generalization of that described in §2, using a space-time grid based on the variables $(x-ct) \cos \alpha + y \sin \alpha$, $x-ct$. A detailed comparison with the wave solutions of Saffman & Yuen (1980) could not be made because their weakly nonlinear perturbation expansion assumes that the direction in which the shape of the doubly periodic wave remains constant coincides with the unperturbed Stokes wave direction. Doubly periodic waves near the right boundary in figure 2 have constant shape in a frame of reference moving in the x -direction, while the Stokes waves from which they bifurcate move at angles θ_0 with the x -direction. It has not been possible to find, by the present numerical method, fully nonlinear doubly periodic waves whose direction of constant shape coincides with the direction of the unperturbed Stokes waves from which they bifurcate.

The occurrence of different forms for doubly periodic waves illustrates the known property that the nonlinear dispersion relation for waves in two horizontal directions on deep water admits many possibilities for resonance and for locking together of wave components.

REFERENCES

- BRYANT, P. J. 1984 Oblique wave groups in deep water. *J. Fluid Mech.* **146**, 1–20.
 LIGHTHILL, J. 1978 *Waves in Fluids*. Cambridge University Press.
 MA, Y.-C. 1982 On steady three-dimensional deep water weakly nonlinear gravity waves. *Wave Motion* **4**, 113–125.
 MARTIN, D. U. 1982 Two-dimensional bifurcations of Stokes waves. *Wave Motion* **4**, 209–219.
 MCLEAN, J. W. 1982 Instabilities of finite-amplitude water waves. *J. Fluid Mech.* **114**, 315–330.

- MCLEAN, J. W., MA, Y. C., MARTIN, D. U., SAFFMAN, P. G. & YUEN, H. C. 1981 Three-dimensional instability of finite-amplitude water waves. *Phys. Rev. Lett.* **46**, 817–820.
- MEIRON, D. I., SAFFMAN, P. G. & YUEN, H. C. 1982 Calculation of steady three-dimensional deep-water waves. *J. Fluid Mech.* **124**, 109–121.
- ROBERTS, A. J. 1983 Highly nonlinear short-crested water waves. *J. Fluid Mech.* **135**, 301–321.
- ROBERTS, A. J. & PEREGRINE, D. H. 1983 Notes on long-crested water waves. *J. Fluid Mech.* **135**, 323–335.
- ROBERTS, A. J. & SCHWARTZ, L. W. 1983 The calculation of nonlinear short-crested gravity waves. *Phys. Fluids* **26**, 2388–2392.
- SAFFMAN, P. G. & YUEN, H. C. 1980 A new type of three-dimensional deep-water wave of permanent form. *J. Fluid Mech.* **101**, 797–808.
- SU, M.-Y. 1982 Three-dimensional deep-water waves. Part 1. Experimental measurement of skew and symmetric wave patterns. *J. Fluid Mech.* **124**, 73–108.